2015 IEEE Conference on Control Applications (CCA)
Part of 2015 IEEE Multi-Conference on Systems and Control
September 21-23, 2015. Sydney, Australia

Mitigating Rotational Disturbances on a Disk Drive with Mismatched Linear Accelerometers

Daniel Y. Abramovitch*

George Hsu**

Abstract— **Hard disk drives still form the backbone of the data storage business. While hard disks have been phased out of portable applications by solid state drives (SSDs), rotating media hard disks are still heavily used in data server farms. These disks, being tightly packed together are affected by external vibrations from their neighboring drives. These vibrations induce increased Position Error Signal (PES). As described in [1], [2], the samples on hard disks are limited, limiting the disturbance cancellation using just the main tracking loop. In [1] an adaptive feedforward method was used to significantly reduce the effects of rotational disturbances using an auxiliary signal from a rotary accelerometer. However, the push for lower costs has meant that rather than a perfectly calibrated rotary accelerometer, server drives typically difference the signals from two linear accelerometers which are often slightly mismatched. The mismatch limits the utility of the rotary feedforward signal. This paper describes an algorithm which solves the problem by calibrating not only the needed accelerometer feedforward gain, but the mismatch between the two linear accelerometers [3].**

I. Introduction

Accelerometer feedforward for disturbance rejection in disk drives is not a new topic. Since the time that the rotary actuators became mechanically balanced, the focus has been on rejecting rotational shock and vibration [4], [5]. The paper by Davies and Sidman [6] gave conditions for exact accelerometer feedforward cancellation of rotary disturbances. White and Tomizuka [4] showed how to adaptively filter complex head disk assembly (HDA) mechanics. Even then, drive to drive variation means that the rotary accelerometer feedforward must be adaptive, and adaptation algorithms carried out when there is insufficient stimulus will track noise and not have parameter convergence. The work in [2] overcame the fundamental sampling limit imposed by sectored servos by sampling the rotary accelerometer signal at a sample rate several times higher than the position control loop. Finally, the cost of using a rotary accelerometer or manually matching a pair of linear accelerometers is an issue, since rotary feedforward correction from a difference mismatched linear accelerometers leads to spurious signals from translational acceleration being used in rotary feedforward. A gain variation of $\pm 15\%$ can significantly decrease the effectiveness of accelerometer feedforward compensation [7].

For this reason, many of the patents in this area go out of their way to determine if the detected rotary acceleration signal is large enough to be useful in feedforward in spite of the unwanted bleed-through from translational acceleration [8], [9] or switch to a back EMF sensing scheme to avoid accelerometer mismatch altogether [10], [11]. Finally, the algorithms for adaptive feedforward correction are often computationally too expensive to put in a disk drive.

This paper solves all of these problems, building on the work in [2]. It makes use of the multirate control and simple adaptation, but adds a second adaptive loop to calibrate the two linear accelerometers. It also improves on the signal detection so adaptation only happens when the accelerometer signals have sufficient amplitude. The algorithm is quite simple and allows for feedforward compensation of rotary disturbances to be used even when the disturbance is small. The algorithm can be implemented as an add on to an existing control scheme or folded into the drive controller itself.

II. Modeling Disturbances into the Disk Drive

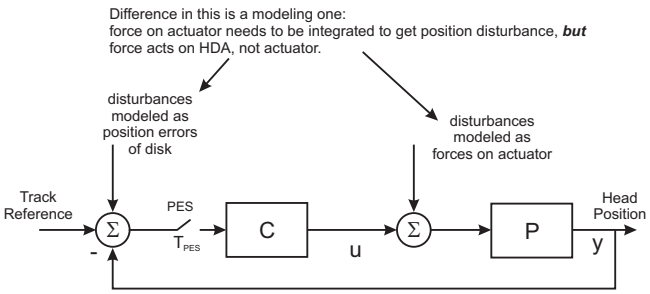

Fig. 1. Modeling disturbances entering the disk drive control loop.

To develop an algorithm, we must model a disturbance on the HDA and how it affects the Position Error Signal (PES) in the tracking control loop. We do this as a transfer function form the disturbance into PES, as shown in Figure 1, in contrast to modeling it as a force into the actuator, P. This is more physically close to reality, since the disturbance generally acts through the HDA to move the disk out from under the head.

- Disturbance is modeled as acceleration entering as a disturbance into PES.
- Ideally, we can model as a transfer function from acceleration to PES, F_{HDA}.
- The acceleration disturbance acting on the HDA will have translational and rotational components, i.e., $a_D = a_R + a_T$.
- The response to each of these components will be different.
- For most drives, a_R has a much bigger effect than a_T.

*Daniel Y. Abramovitch is a system architect in the Mass Spectrometry Division, 5301 Stevens Creek Blvd., M/S: 3U-DG, Santa Clara, CA 95051 USA, danny@agilent.com

**George Hsu is CEO of PNI Sensors Corporation. This work was done for Sensor Platforms, Inc. (SPI), which has since been acquired by Audience.com. ghsu@pnicorp.com

III. The Classic Disk Feedforward Problem

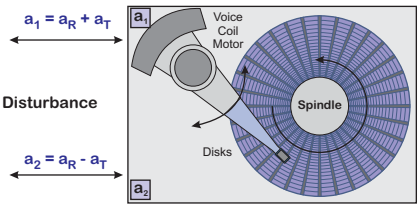

Fig. 2. Using two linear accelerometers on a head disk assembly (HDA).

In Figure 2, a pair of linear accelerometers, placed on the HDA are differenced to form a rotational signal. This is done because a perfectly calibrated rotational accelerometer is expensive and is often less sensitive than differencing a pair of linear accelerometers at opposite sides of the HDA. The linear accelerometers are often slightly mismatched, in that they share dynamics but have gain variations up to about 15% [7]. Still, a pair of accelerometers can be used to estimate physical accelerations. The feedforward control from the accelerometers is often in a conceptually separate block from the main tracking loop. The characteristics of this problem are:

- The drive loop is almost always sectored servo with sample period, T.
- The feedforward controller takes 2 sensors, sampled at T/M, and computes a signal to be injected at the feedforward input of the drive loop.
- Often a fixed filter is used for the sensors.
- The adaptation is done on the filter/feedforward gains.

IV. Current Methods and Limitations

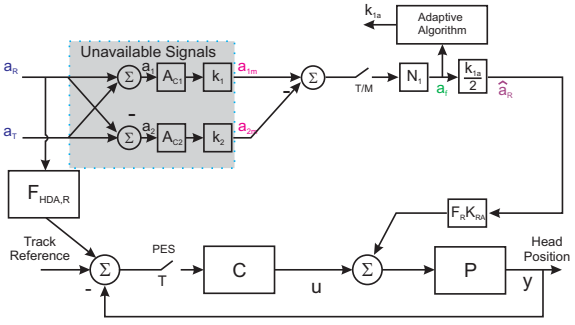

Fig. 3. Accelerometer feedforward done with simplifying assumptions.

Figure 3 shows an accelerometer feedforward loop into a disk drive where the two linear accelerometers are summed before being sampled. The compensating digital filter, N_1, is used on the combined accelerations to compensate for the accelerometer responses. In this model, the underlying assumption is that the transfer function from a_T, into PES is negligible and the linear accelerometer signals are matched, so that $N_1(z) \sim A_{C1}^{-1}(z) = A_{C2}^{-1}(z)$. The accelerometer measurements can be combined in analog circuitry, giving the estimated a_R via:

$$\hat{a}_R = \frac{k_{1a}}{2}\left(k_1 a_1 - k_2 a_2\right), \tag{1}$$

a_R	a_T	% Gain Mismatch	a_1	a_2	$\frac{a_1 - a_2}{2}$
0.5	10	0%	10.50	9.50	0.5
0.5	10	1%	10.55	9.45	0.55
0.5	10	2%	10.6	9.4	0.6
0.5	10	3%	10.66	9.36	0.65
0.5	10	4%	10.7	9.3	0.7
0.5	10	5%	10.76	9.26	0.75
0.5	20	5%	21	19	1

TABLE I

Effects of accelerometer mismatch.

where the accelerometer gains k_1 and k_2 are unknown but assumed to be matched, and the adjustment of k_{1a} scales the feedforward signal so that the effects of a_R are decorrelated from PES. If we go through the math from [6] or [1] we see that our accelerometer equalizing filter N_1 has the shape:

$$N_1 = \frac{F_{R,HDA}}{A_{C1}P} = \frac{F_{R,HDA}}{A_{C2}P}. \tag{2}$$

The gain adjustment of k_{Ra} can be part of k_{1a} so that we can set $k_{Ra} = 1$. As for the ratio of $F_{R,HDA}$ and P, accelerometer feedforward is typically applied in the frequency range of 100 Hz to 1 kHz. Below that, the main tracking loop can handle the disturbance. Above that does not seem to be a problem, probably because of the low pass nature of $F_{R,HDA}$. What this means is that in the frequencies of interest, both P and $F_{R,HDA}$ can be modeled as double integrators, which means that their ratio is yet another gain which can be compensated with our adaptive k_{1a} The use of a fixed filter to adjust the responses has been discussed in several sources [1], [2], [4], [7], [12], [13].

The main issue with the model of Figure 3 is that it cannot compensate for gain mismatches between the two accelerometers, which causes bleeding of translational disturbance into the measured rotational disturbance. This is shown in Table I. With strong enough translational disturbances, even a 5% mismatch creates a much larger apparent rotational acceleration. Since the drive is (to first order) immune to translational disturbances, mismatch leads to offtrack even when $a_R = 0$. Many algorithms to try to limit accelerometer feedforward to cases when it seems to help, i.e., large sensed rotational disturbances [8], [9]. In contrast, the algorithm here uses this bleeding in of translation to calibrate the relative gain of the two accelerometers.

V. Algorithms to Adaptively Balance Signals

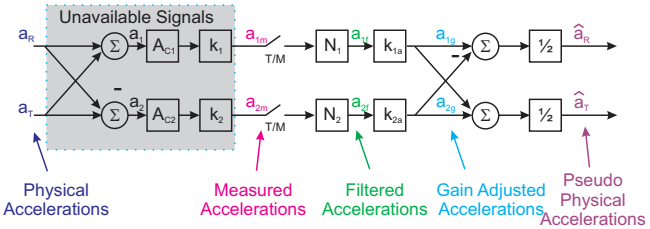

Fig. 4. Sensing rotation and translation

Consider two accelerometers on the same axis, as shown in Figure 2. The structure is accelerated both in translation perpendicular to that axis and in rotation. So each accelerometer ideally sees

$$a_1 = a_T + a_R \text{ and } a_2 = a_T - a_R \tag{3}$$

where a_T is the translational acceleration and a_R is the rotational acceleration. So, if we had these ideal measurements then

$$a_T = \frac{a_1 + a_2}{2} \text{ and } a_R = \frac{a_1 - a_2}{2} \tag{4}$$

We don't have access to a_1 and a_2, only $a_{1m} = k_1 a_1$ and $a_{2m} = k_2 a_2$ where k_1 and k_2 are not known. The best estimates of a_R and a_T are

$$\hat{a}_R = \frac{k_{1a} a_{1m} - k_{2a} a_{2m}}{2} \text{ and } \hat{a}_T = \frac{k_{1a} a_{1m} + k_{2a} a_{2m}}{2}, \tag{5}$$

which after some algebra can be reformulated as:

$$\hat{a}_R = \frac{k_{1a}k_1 - k_{2a}k_2}{2} a_T + \frac{k_{1a}k_1 + k_{2a}k_2}{2} a_R, \tag{6}$$

$$\hat{a}_T = \frac{k_{1a}k_1 + k_{2a}k_2}{2} a_T + \frac{k_{1a}k_1 - k_{2a}k_2}{2} a_R. \tag{7}$$

Our desired feedforward signal, which is proportional to $\hat{a}_R$, has both true rotational acceleration, a_R, and true translational acceleration, a_T, unless our gains are properly matched. With matched accelerometer gains, $\hat{a}_R$, works ideally when $k_{1a} = \frac{1}{k_1}$ and $k_{2a} = \frac{1}{k_2}$. However, since we don't know k_1 and k_2, we have to figure things out from the decorrelation with the PES signal. Ideally, a_T is orthogonal to PES and when it is fed into the system with the right gain, this will be true. $\hat{a}_R$ and $\hat{a}_T$ are "pseudo-physical signals" or estimated physical accelerations, and can used in the adaptation. They are diagrammed in Figure 4.

Also, we will assume that in the frequency range of interest

$$N_1(z) = A_{C1}^{-1}(z) \tag{8}$$

and

$$N_2(z) = A_{C2}^{-1}(z). \tag{9}$$

Thus, we use the fixed filters, N_1 and N_2, to equalize the effect of the accelerometer dynamics, A_{C1} and A_{C2}.

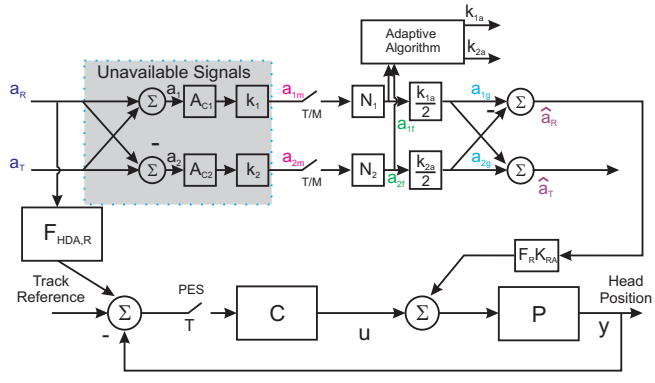

Fig. 5. Adaptive feedforward structure to balance k_{1a} and k_{2a}.

Looking at Figure 5, we note that we have assumed $F_{HDA,T} = 0$, at least to first order, so there is no intentional feedforward control from a_T. The transfer function from a_R to PES can seen to be

$$\frac{PES}{a_R} = \frac{F_{R,HDA}}{1+PC} - \frac{k_1 k_{1a} k_{Ra} F_R P}{1+PC} - \frac{k_2 k_{2a} k_{Ra} F_R P}{1+PC}. \tag{10}$$

We can filter this further by setting $k_{Ra} = 1$

$$\frac{F_{R,HDA}}{1+PC} = \frac{F_R P}{1+PC} \triangleq H_1. \tag{11}$$

So now,

$$\frac{PES}{a_R} = H_1 \left[1 - k_1 k_{1a} - k_2 k_{2a}\right]. \tag{12}$$

Similarly, the transfer function from a_T to PES is simplified with $F_{T,HDA} = 0$ and $F_T = F_R$ so that

$$\frac{PES}{a_T} = -H_1 \left[k_1 k_{1a} - k_2 k_{2a}\right]. \tag{13}$$

Combining these we have

$$\begin{aligned} PES = \; & H_1 \left[a_R - \left(k_1 k_{1a} + k_2 k_{2a}\right) a_R \right. \\ & \left. - \left(k_1 k_{1a} - k_2 k_{2a}\right) a_T\right] \end{aligned} \tag{14}$$

The transfer functions between external acceleration and PES are zero if

$$\frac{PES}{a_T} = 0 \text{ if } k_{1a}k_1 - k_{2a}k_2 = 0 \text{ and} \tag{15}$$

$$\frac{PES}{a_R} = 0 = \frac{F_{R,HDA} - F_R(k_{1a}k_1 + k_{2a}k_2)P}{1+PC}. \tag{16}$$

Equation 15 indicates that we have properly matched the accelerometer gains. In Equation 16, the matching condition that nulls the effect of a_R on PES is that we match both the magnitude and phase of F_{HDA} with our fixed filter, F, our scaled accelerometer signals, $k_{1a}k_1 + k_{2a}k_2$, and the disk actuator model, P. Our scaled accelerometer signals only account for a gain matching condition. We need the equalizing filter, F_R, to match the phase of the effect of rotary acceleration on the disk drive.

VI. Adapting k_{1a} and k_{2a}

A search algorithm, such as the Least Mean Squares (LMS) algorithm [14], is generated by using some set of derivatives of a cost function. For Equation 14, we have two weights to adapt, $w_0 = k_{1a}$ and $w_1 = k_{2a}$. The error that we are trying to minimize in a least squares form is PES. So, we need the gradient of PES with respect to each of the weights:

$$\frac{\partial PES}{\partial k_{1a}} = -H_1 \left[k_1 a_R + k_1 a_T\right] \tag{17}$$

$$= -H_1 k_1 \left[a_R + a_T\right] = -H_1 k_1 a_1 \tag{18}$$

$$= -H_1 a_{1m}. \tag{19}$$

Likewise,

$$\frac{\partial PES}{\partial k_{2a}} = -H_1 \left[k_2 a_R - k_2 a_T\right] \tag{20}$$

$$= H_1 k_2 \left[a_T - a_R\right] = H_1 k_2 a_2 \tag{21}$$

$$= H_1 a_{2m}. \tag{22}$$

The filter, H_1 filters all the signals in Equation 14, so it does not change the adaptation. This filter represents a fixed filter which matches the response of the feedforward signal to the PES signal.

The adaptation for k_{1a} and k_{2a} is based on the two signals $a_{1m} = k_1 a_1$ and $a_{2m} = k_2 a_2$. We do not know k_1 and k_2, so we have to work to decouple their effect on PES. So, now, following the negative of the gradient, the parameter update is:

$$k_{1a}(i+1) = k_{1a}(i) + 2\mu_1 PES(i) a_{1m}(i) \quad (23)$$
$$k_{2a}(i+1) = k_{2a}(i) - 2\mu_2 PES(i) a_{2m}(i) \quad (24)$$

Recalling Equations 6 and 7, we see that with gains properly tuned, $k_{1a} \approx \frac{1}{k_1}$ and $k_{2a} \approx \frac{1}{k_2}$ so that, $\hat{a}_R \approx a_R$ and $\hat{a}_T \approx a_T$. The parasitic feedthrough from a_T has been eliminated.

VII. Adapting k_{1a} and k_{3a}

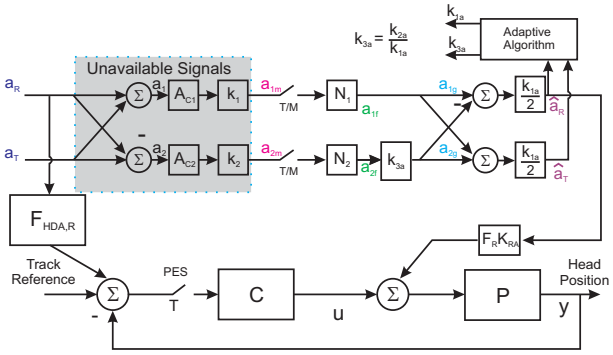

Fig. 6. Adaptive feedforward structure to balance k_{1a} and k_{3a}.

An alternate form that adapts on inputs from $\hat{a}_R$ and $\hat{a}_T$ is shown in Figure 6. k_{1a} and k_{3a} will adapt to balance the two accelerometer paths so that no bleeding of a_T into feedforward signal is stopped. Here, $k_{3a} = k_{2a}/k_{1a}$, but this alternate factorization lets us work on the estimated physical accelerations directly.

$$k_{1a}(i+1) = k_{1a}(i) + 2\mu_R PES(i) \hat{a}_R(i) \quad (25)$$
$$k_{3a}(i+1) = k_{3a}(i) - 2\mu_T PES(i) \hat{a}_T(i). \quad (26)$$

The two adaptation loops adapt the two separate adaptive gains, k_{1a} and k_{3a}. As before, the action is to null the parasitic path from a_T to PES so that the feedforward from a_R to PES can do its job.

$$\hat{a}_R = \frac{k_{1a}}{2}\left(k_1 a_1 - \frac{k_{2a}}{k_{1a}} k_2 a_2\right) \quad (27)$$

and

$$\hat{a}_T = \frac{k_{1a}}{2}\left(k_1 a_1 + \frac{k_{2a}}{k_{1a}} k_2 a_2\right). \quad (28)$$

With $N_1 \approx A_{C1}^{-1}$ and $N_2 \approx A_{C2}^{-1}$ we end up with

$$\hat{a}_R = \frac{k_{1a}}{2}\left(\left(k_1 - \frac{k_{2a}}{k_{1a}} k_2\right) a_T + \left(k_1 + \frac{k_{2a}}{k_{1a}} k_2\right) a_R\right) \quad (29)$$

and

$$\hat{a}_T = \frac{k_{1a}}{2}\left(\left(k_1 + \frac{k_{2a}}{k_{1a}} k_2\right) a_T + \left(k_1 - \frac{k_{2a}}{k_{1a}} k_2\right) a_R\right). \quad (30)$$

With gains properly tuned, $k_{1a} \approx \frac{1}{k_1}$ and $k_{2a} \approx \frac{1}{k_2}$ so that $\hat{a}_R \approx a_R$ and $\hat{a}_T \approx a_T$.

VIII. Switching Algorithms On and Off

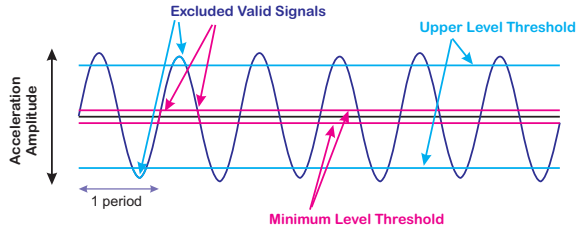

Fig. 7. Diagram showing large amplitude signals that may have exclusion zones with simple level detection.

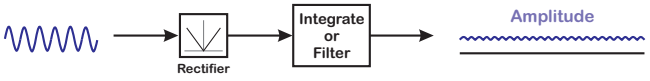

Fig. 8. Simple amplitude detection.

It is well understood that adapting when signal levels are low and have bad SNR leads to poor adaptation and potentially bad results. On the other hand, signals that are too large may saturate or may be due to a seek operation. In prior art, some signal level detection was used to limit adaptation to times when signals were above some minimum level threshold, as shown in Figure 7. However, simply cutting off all signals below that level means that for a sinusoidal signal such as what is shown in Figure 7, significant sections of a perfectly reasonable signal are excluded from adaptation. The algorithms here use amplitude detection, in the form of a "rectify and filter" scheme shown in Figure 8. In actual usage, the frequency content of the disturbance is unknown a priori, so coherent demodulation is not an option. The rectify and filter approach produces an estimate of the baseband amplitude. When the estimated amplitude is out of range, we shut off adaptation. A separate range can be used for turning the feedforward on and off, but removing effects of a_T substantially reduces the need for this. This approach is very effective and computationally simple.

IX. Simulation and Measurement Results

A basic disk drive tracking model was constructed using Simulink to test the algorithm. The model featured a simple double integrator form for the actuator, a PID controller, and a disturbance transfer function model into the PES. The model was thoroughly stimulated with alternate levels of a_R and a_T, either as purely random (Figures 9 and 10) or the more difficult intermittent sinusoidal disturbances (Figures 11 and 12). The former showed the basic operation of the adaptation loops, while the latter showed the adaptation loops combined with the algorithms to switch adaptation on and off, as described in Section VIII.

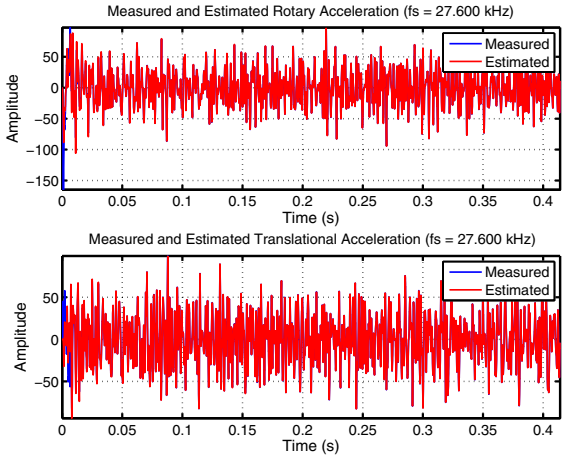

Fig. 9. Adaptation simulation using noise driven a_R and a_T, i.e. a_R and a_T are driven by noise only. The parameters adjust to minimize PES. Mismatch in estimated and actual accelerations are found only at the beginning of adaptation. A noise scaling of 4 on both a_R and a_T was used.

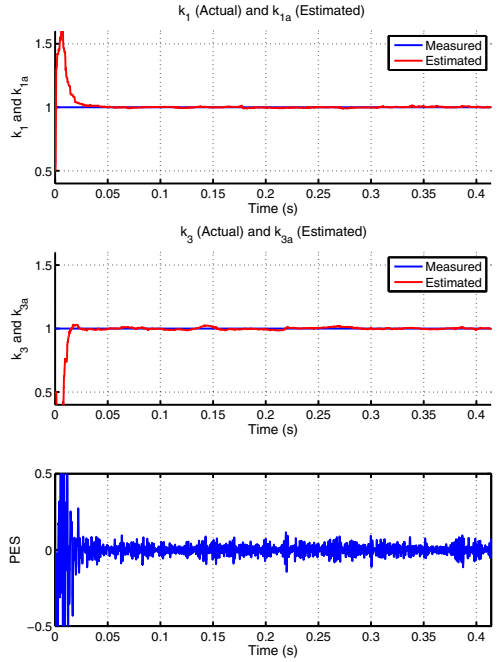

Fig. 10. Adaptation simulation of Figure 9. The initial gain estimates were off by 50%, i.e., $k_1 = 1$ (actual) while $k_{1a}(0) = 0.5$ (initial estimate) and $k_3 = 1$ (actual) while $k_{3a}(0) = 0.5$ (initial estimate). Note the rapid convergence of k_{1a} to k_1 and k_{3a} to k_3. The effects of disturbance on PES rapidly goes away.

Following that, the algorithms were implemented by Dave Hammil in DSP on an emulation system at SPI, built by Eric Miller and Carol Wilson, and shown in Figure 13. On the left is a block diagram showing the layout of the system implemented in the picture on the right. Central to this test system is the shaker that consists of two linear actuators that can be driven by a combination of in-phase and out of phase signals so as to generate translational and rotational shaking. Above the two actuators is a bridge structure that holds the drive and other sensors, and these are connected to the shakers through flexures. The response of the shaker

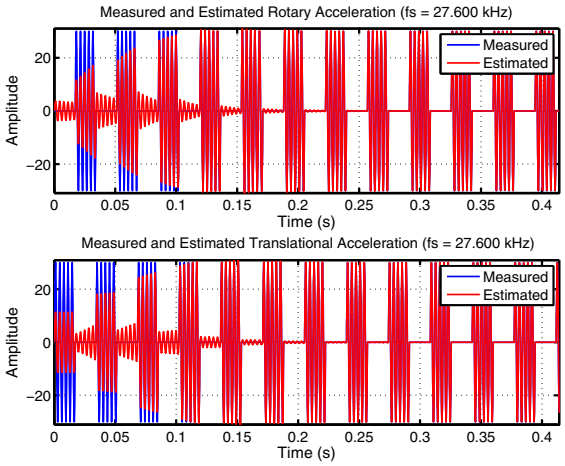

Fig. 11. Adaptation simulation where a_R and a_T are driven by intermittent sine waves. The parameters adjust to minimize PES. Mismatch in estimated and actual accelerations are found only at the beginning of adaptation. Intermittent sine waves at 300 Hz and amplitude 30 were injected into a_R and a_T. The amplitude detection only allowed adaptation when there was usable signal on which to adapt.

to vibration can be measured by using extra laboratory grade calibrated accelerometers on the bridge structure. The shaker response is shown in Figure 14, and it shows that the shaker itself has a resonance. The drive Position Error Signal (PES) in response to varying levels of rotational vibration is shown in Figure 15. The algorithm as implemented reduces sensitivity of PES to rotational vibration by 15-20 dB over a frequency span of 450 Hz to 1100 Hz.

After verifying their performance, the algorithms were put into Silicon with the SPI 1235 chip. The chip is designed as a drop in solution for drive manufacturers, an auxiliary controller that needs only PES and seek signals to guide the tuning. The resulting auxiliary control signal is summed in after the drive DAC. The SPI 1235 algorithms covered by US Patent 7,768,783 [3], so they could be directly licensed to drive manufacturers for implementation inside their own control processors.

X. Conclusions

The algorithms presented here are highly effective and simple to implement in real time. They present a highly practical extension to the author's previous work in the area, in that less expensive, uncalibrated linear accelerometers can now replace rotary accelerometers. The addition of the second adaptation path to balance the two accelerometer signals dramatically simplifies the use of adaptive feed-forward for this drives since complicated algorithms are no longer needed to determine if the rotary acceleration estimate is good enough to use. Furthermore, the simple amplitude demodulation allows the algorithm to only adapt when there is sufficient signal level to assure adaptation. The algorithms are simple and effective, because they attack the fundamental weakness of accelerometer feedforward in disk drives, unbalanced sensors, and only do adaptation when there is high enough signal level for adaptation to work well.

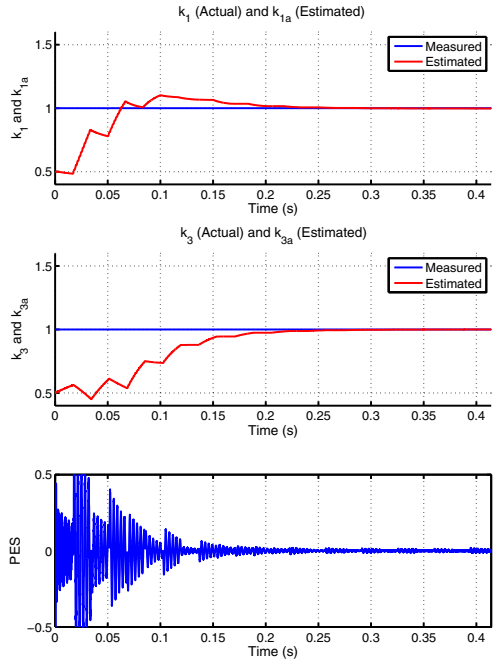

Fig. 12. Adaptation simulation of Figure 11. The initial gain estimates were off by 50%, i.e., $k_1 = 1$ (actual) while $k_{1a}(0) = 0.5$ (initial estimate) and $k_3 = 1$ (actual) while $k_{3a}(0) = 0.5$ (initial estimate). Note the rapid convergence of k_{1a} to k_1 and k_{3a} to k_3. The effects of disturbance on PES rapidly goes away.

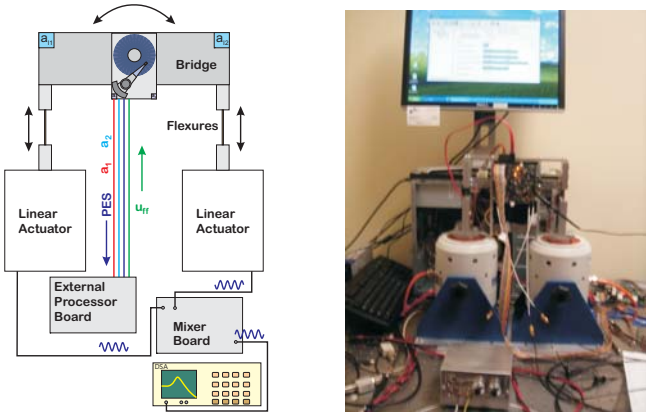

Fig. 13. On left: Block diagram for shaker system. On right, SPI test platform including disk drive, external controller board, and shaker system.

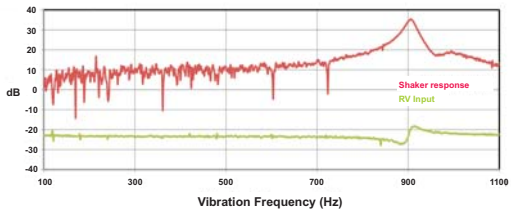

Fig. 14. Bode plot of shaker system response to rotational vibration.

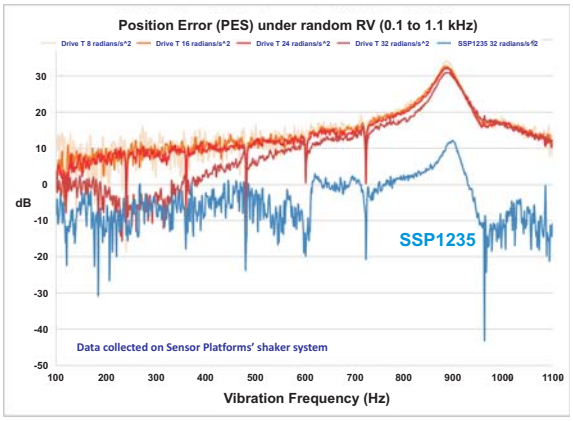

Fig. 15. Response of drives under different levels of rotational vibration.

REFERENCES

[1] D. Abramovitch, "Rejecting rotational disturbances on small disk drives using rotational accelerometers," in *Proceedings of the 1996 IFAC World Congress*, (San Francisco, CA), pp. 483–488 (Volume O), IFAC, IEEE, July 1996.

[2] D. Y. Abramovitch, "Rejection of disturbances on a disk drive by use of an accelerometer," United States Patent 5,663,847, Hewlett-Packard, Palo Alto, CA USA, September 2 1997.

[3] D. Y. Abramovitch and G. Hsu, "Mitigating the effects of disturbances of a disk drive," United States Patent 7,768,783, Sensor Platforms, Inc., San Jose, CA USA, August 3 2010.

[4] M. White and M. Tomizuka, "Increased disturbance rejection in magnetic disk drives by acceleration feedforward control," *Control Engineering Practice*, vol. 5, no. 6, pp. 741–751, 1997.

[5] R. F. Smith, "Apparatus for sensing operating shock on a disk drive," United States Patent 5,235,472, Seagate Technology, Inc., Scotts Valley, CA, August 1993.

[6] D. B. Davies and M. D. Sidman, "Active compensation of shock, vibration, and wind-up in disk drives," in *Proceedings of the 1991 ASME Winter Annual Meeting*, ASME, November 1991.

[7] A. Jinzenji, T. Sasamoto, K. Aikawa, S. Yoshida, and K. Aruga, "Acceleration feedforward control against rotational disturbance in hard disk drives," *IEEE Transactions on Magnetics*, vol. 37, pp. 888–893, March 2001.

[8] T. Semba, M. T. White, and K. I. Tzou, "Magnetic recording disk drive with switchable rotational vibration cancellation," United States Patent Application US2007/0030768, Hitachi Global Data Storage, San Jose, CA USA, February 8 2007.

[9] A. Narayana, R. Codilian, and L. V. Ngo, "Vibration cancellation in a disk drive by using an acceleration sensor and adaptively adjusting its gain to minimize external acceleration effects," United States Patent 6,914,743, Western Digital Technologies, Lake Forest,CA USA, July 5 2005.

[10] S. M. Sri-Jayantha, H. Dong, V. D. Khanna, G. McVicker, and M. Ohta, "Rotational vibration velocity-based sensor for disk drives," United States Patent 6,963,463, Hitachi Global Data Storage, San Jose, CA USA, November 8 2005.

[11] S. M. Sri-Jayantha, H. Dong, A. Sharma, and I. Yoneda., "Method and system for rotational velocity-based algorithm for vibration compensation in disk drives," United States Patent 6,898,046, Hitachi Global Data Storage, San Jose, CA USA, May 24 2005.

[12] D. Abramovitch, "Rejecting rotational disturbances on small disk drives using rotational accelerometers," *Control Engineering Practice*, vol. 5, November 1997.

[13] M. White and M. Tomizuka, "Increased disturbance rejection in magnetic disk drives by acceleration feedforward control," in *Proceedings of the 1996 IFAC World Congress*, (San Francisco, CA), pp. 489–494 (Volume O), IFAC, IEEE, July 1996.

[14] B. Widrow and S. D. Stearns, *Adaptive Signal Processing*. Englewood Cliffs, New Jersey: Prentice-Hall, 1985.